

CHAPTER 10

THERMOELECTRIC STUDIES OF Sb_2Te_3 AND Sb_2Te_3 BASED ALLOY CRYSTALS

To determine the usefulness of any semiconductor as a thermoelectric material the “figure of merit” Z , is evaluated for which the knowledge of electrical conductivity, Seebeck coefficient and thermal conductivity is must. Other conditions being equal, the efficiency of the thermoelectric device increases with Z . Electrical conductivity experiments at very low temperatures (down to the order of 1°K) have proved extremely fruitful for the understanding of many aspects of electrical conduction and the properties of conductors in general. The interest in thermal conductivity was at first less intense (partly because it is rather more difficult to measure with accuracy), but within the last twenty years or so interest in thermal conductivity has increased very much. Seebeck coefficient measurement is the simplest measurement to carry out since it does not require the application of good electrical contacts which for most semiconductors are not simple enough.

There are many reports^[1-26] of the thermoelectric measurements on Sb_2Te_3 , $\text{Sb}_2\text{Te}_3\text{-Bi}_2\text{Te}_3$ and doped antimony telluride prepared under different conditions; e.g. directional freezing^[1-3], Bridgman method^[4-9], Zone Melting^[8], Travelling Heater Method^[10], Czochralskii method^[11-16], ultrarapid cooling of melts^[17], extruded solid solution^[18-20] sintered solid solutions^[21,22] and Zone recrystallization^[26].

Alieva et al.^[1,2] have studied the influence of surface treatment of crystals of solid solutions of the $\text{Bi}_2\text{Te}_3\text{-Bi}_2\text{Se}_3$ and $\text{Bi}_2\text{Te}_3\text{-Sb}_2\text{Te}_3$ systems on their thermoelectric properties. In [1] they have shown that the treatment of the surfaces significantly alters thermoelectric efficiency of the Bi_2Te_3 based solid solutions while in [2] they have revealed the mechanism of these changes. Reinshaus et al.^[3]

have investigated the macrosegregation of tellurium in normal freezed BiSbTe₃ crystals by the thermoprobe technique. In references 4-6, 15 and 16, the influence of impurities on the thermoelectric properties of Sb₂Te₃ crystals have been studied. Zeinalov et al.^[7] have studied the influence of radiation on the thermal conductivity of Bi₂Te₃-Sb₂Te₃ and Bi₂Te₃-Bi₂Se₃ solid solutions, measured by an absolute steady state method. Ha et al.^[8] have studied the effect of excess tellurium on the thermoelectric properties of Bi₂Te₃-Sb₂Te₃ solid solutions. They have observed an increase in the electrical resistivity after annealing and have attributed this effect to a decrease in concentration of antistructural defects within the major phase and not to the presence of the Te second phase. Cosgrove et al.^[9] have observed the effect of freezing conditions on the thermoelectric properties of Bridgman grown BiSbTe₃ crystals.

Ivanova et al.^[11,12] have assessed the inhomogeneity of Czochralski-grown crystals of Bi₂Te₃-Sb₂Te₃ solid solutions by measuring the longitudinal and cross-sectional distributions of thermoelectric power. The most non-uniform cross-sectional distributions of thermoelectric power were observed at the ends of the crystal. Thermoelectric properties are found to depend substantially on growth conditions and a decrease in longitudinal inhomogeneity was obtained by varying the pulling rate during growth^[11]. It has been shown^[12] that heat treatment of samples cut from various parts of the crystal can reduce radial inhomogeneity. These authors have also studied the homogeneity of Bi_{0.5}Sb_{1.5}Te₃ single crystals^[13] grown at various rotation rates of the crucible and the ingot. As the crucible rotation rate is increased from 6 to 15 rpm, the spread in thermopower over the crystal slice is reduced by half.

The electrical properties of the extruded samples of Bi₂Te₃-Sb₂Te₃ have been studied^[19,20] and it has been observed that the performance at low temperatures is slightly poorer than that of the samples obtained by directional crystallization and is 20-40% higher than that of the pressed ones. Amin et al.^[22] have studied the thermoelectric properties of Bi₂Te₃ based -p and -n type alloys

prepared by either cold pressing and sintering or hot pressing. They have shown that the figure of merit for the finest grain size is almost the same as the best crystal value which is due to the decrease of thermal conductivity caused by scattering of phonons at grain boundaries for grain sizes comparable to the mean free path of phonons.

Glazov et al.^[23,24] have investigated the electrical properties of compounds Bi_2Te_3 , Sb_2Te_3 and Bi_2Se_3 in the region of melting and the liquid state and have shown that the melting process is accompanied by significant metallization of the bonds, giving rise to the semimetallic nature of the alloys of these materials, and in addition, the degree of metallization of the bonds increases in the order $\text{Bi}_2\text{Se}_3 \rightarrow \text{Sb}_2\text{Te}_3 \rightarrow \text{Bi}_2\text{Te}_3$. They have also studied the thermoelectric behavior of the solid solution prepared by ultrafast cooling^[17] and found higher $\alpha^2\sigma$ values as compared to the starting thermoelectric material, where α = thermopower and σ = electrical conductivity. Khvostantsev et al.^[25] have made thermoelectric and relative electroresistance measurements on Sb_2Te_3 single crystals under hydrostatic pressure upto 9 GPa and temperatures upto 400°C and found that changes of kinetic coefficients are attributable to the formation of three high pressure phases of Sb_2Te_3 .

In the present work an investigation of the influence of Bi and In atoms, incorporated in the Sb_2Te_3 lattice, on electrical and thermal conductivities and Seebeck coefficient, was carried out with an aim to ascertain the effect of impurity and its concentration variation on the thermoelectric figure of merit. A discussion of experiments and results follows.

SAMPLE PREPARATION

Sb_2Te_3 and Bi_2Te_3 have layered rhombohedral structures built up of sandwiches of five atomic layers in the sequence $\text{Te}^1\text{-M-Te}^2\text{-M-Te}^1$ ($\text{M} = \text{Sb, Bi}$)^[27]. Van der Waals-like bonds predominate between the sandwiches, while within the sandwich, the in-layer bonds are saturated, predominantly covalent,

with a small contribution of ionic bonding. As a result, these crystals exhibit easy cleavage.

In the present case, the as-grown single crystals could be easily cleaved (along the (111) plane) always parallel to the direction of pulling, i.e., the ampoule axis. Hence, the cleavage planes were used as the working planes for electrical conductivity measurements. However, for the thermopower and thermal conductivity measurements, the samples were cut in the form of a cylindrical rod of diameter $\sim 10\text{mm}$ by means of a wheel cutter, Model 660 South Bay Technology Inc., in a direction perpendicular to the ampoule axis of the crystal. This was to define uniform cross-section normal to heat flow. Since maximum homogeneity is observed in the central part of the crystal, only the central portion of the crystal, $\sim 6\text{mm}$ long, was used in the investigation while both the ends of the crystal were discarded. After the samples were cut, their surfaces were lapped with carborundum as a result of which the surfaces turn planar and dark, uniformly. Then they were polished with polishing alumina. The resulting sample thickness was ~ 4.5 to 5 mm . The area of cross-section of the sample was evaluated and so was the thickness of the sample measured accurately since it is used in the evaluation of thermal conductivity. It is worthwhile to note that the use of a short sample allows equilibrium to be reached reasonably quickly. For thermal conductivity measurements, it is essential that the thermal contact between the sample and the source/ sink should be exceptionally good. This was obtained by interposing layers of glycerine to reduce the thermal resistance.

ELECTRICAL CONDUCTIVITY STUDY

The electrical conductivity measurements on the samples under study were carried out under low and high temperature conditions separately. The Four Probe Technique was used for the electrical measurements as has been described in Chapter 5. Electrical conductivity measurements made on thermoelectric materials set a special problem which is associated with the Peltier and Seebeck effects. The possibility of stray temperature gradients producing thermoelectric voltages that

might be a source of error in electrical resistance measurements has been recognised for a great many years. However, it is usually possible to eliminate their effect by making observations with the electric current flowing successively in opposite directions. When the current flows in one direction the thermoelectric and resistive voltages are additive, while when it flows in the opposite direction they oppose one another.

EXPERIMENTAL SET UP

For Low Temperature Measurement:

The cryostat used consists of a JANIS closed cycle refrigerator (CCR) system. The schematic diagram of the CCR is shown in Fig. 1. It utilises compressed helium gas in a Gifford McMahon (G-M) cooling cycle. In the Gifford McMahon cycle the working gas is pushed to and fro through a regenerator by a displacement piston. The compression is carried out in a compressor at room temperature, separated from the cooling system. In this process no work is done by the system, but a quantity of heat corresponding to the quantity of cold produced is discarded to the exterior in the same way as cold is produced by adiabatic gas expansion on the cold side of the displacement piston. The gas emerging from the system (compressor) therefore has a higher temperature than the gas entering the system. Air cooling or water cooling is employed to remove this heat.

The G-M method has the advantage that apart from the slowly moving displacement piston, it requires no moving parts at low temperatures. The compressor can be operated separately from the actual cooling system. The control valves are also at room temperature. A 2-stage G-M refrigerator enables one to achieve temperatures down to about 10K.

Further features of the cryostat includes a cold head (the part of the cryostat which attains the minimum temperature), sample holder, etc. The unit is attached to either a water-cooled or air-cooled helium compressor by a pair of 10 feet high pressure flex lines.

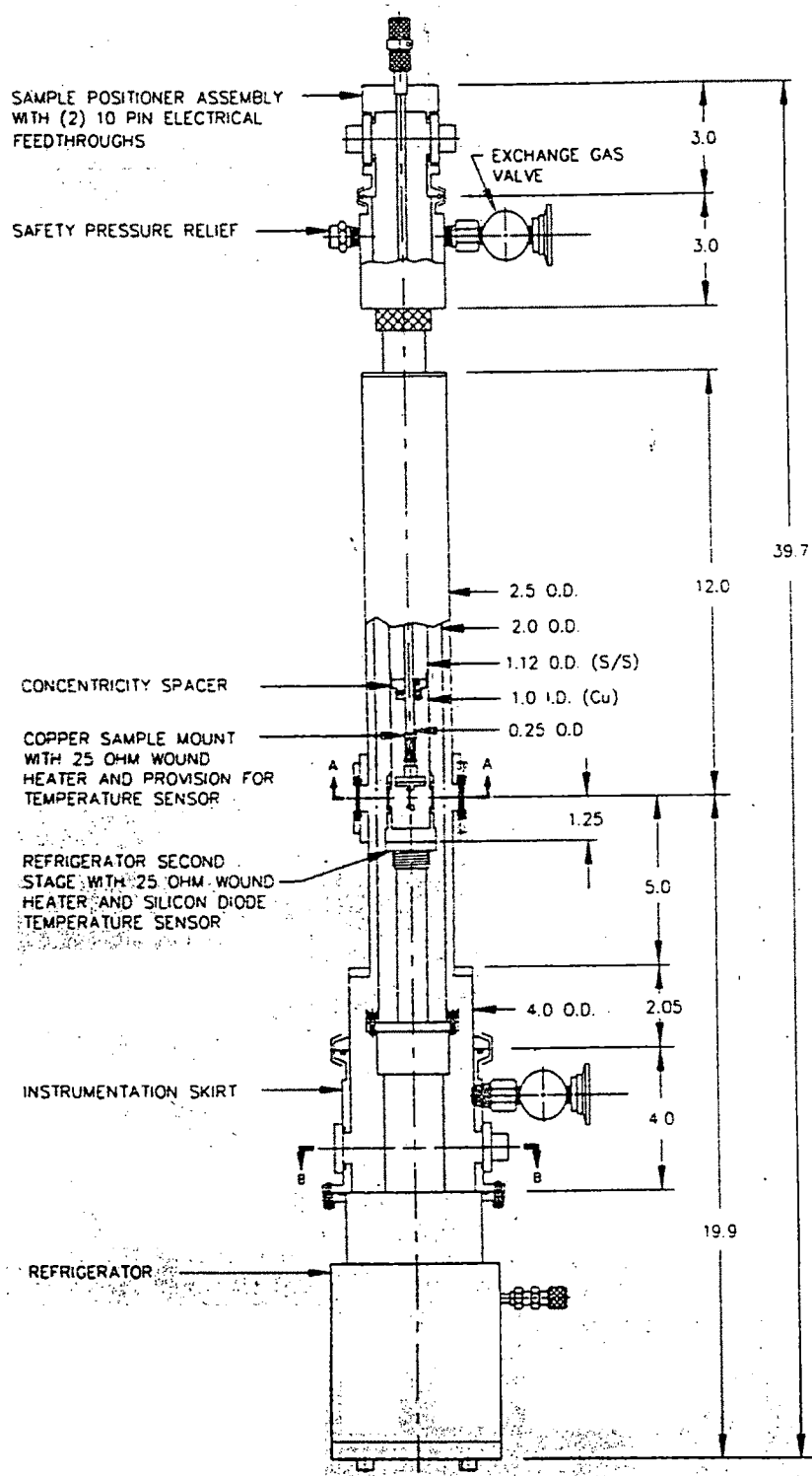


Fig. 1. The schematic diagram of the Closed Cycle Refrigerator

The temperature is varied by means of a bifilarly wound heater attached to the cold finger. The sample mount has a provision for temperature sensors (Lake Shore Si diode is used usually) which, in conjunction with a controller, allows for automatic control of the sample temperature. The temperature controller is usually a Proportional Differential and Integral type. The controller senses the difference in the actual temperature and the Set temperature and differentiates or integrates accordingly.

The DC electrical conductivity measurements of the samples were conducted in the above described cryostat. Vacuum was maintained using a rotary cum diffusion pump. Helium, the exchange gas in the sample chamber provides the thermal contact with the sample.

A platinum resistance thermometer (Pt-100) was used for temperature measurement and the temperature was controlled using a Lake Shore temperature controller. The thermometer was placed on the sample mount [by connecting them using thin copper wires], which was made of copper to provide good thermal connections to the sample. The electrical contacts with the sample were made using silver paint. The sample was attached to the sample holder using GE varnish.

The resistance measurements were made using the DC four probe method. To measure the resistance of the sample, a current in the mA range is sent from an ADVANTEST current source. The total current sent was set to a low value of 1 mA in order to prevent self heating. The voltage drop was measured using a KEITHLEY nanovoltmeter. The current was reversed to check if the same voltage was recorded in the opposite direction.

For High Temperature Measurement:

The Valde's four probe set up is a versatile equipment for the resistivity measurement along plane surfaces of single crystals. This set up is used in the present investigation. In this method all the four probes are directly brought in

pressure contact with the sample. It overcomes several drawbacks of other conventional techniques. The major drawbacks overcome are

- (i) When the electrical contact is taken by directly soldering the conducting material to the sample, the soldering may affect the properties of the sample in the soldered region.
- (ii) When the electrical contact on the sample is taken by either evaporation or any other method, there is always a possibility that a non-ohmic contact is formed. This is undesirable and may influence the measurements significantly.

The four probe arrangement includes an oven, constant current source, milliammeter and a microvoltmeter. The collinear and equally spaced spring loaded four probes are mounted in a teflon bush to insulate them electrically. In addition, a teflon spacer near the tips is also provided to keep the probes equidistant. The whole arrangement is mounted on a suitable stand from where leads for supply of constant direct current and voltage measurement can be taken out. A small oven facilitates measurements at various temperatures above the room temperature. A highly regulated constant current generator ensures desired value of the current that can be controlled through a 100% safety potentiometric arrangement.

The resistivity measurements on the samples carried out using this set up assumes that (i) the resistivity of the sample is uniform in the area of measurements, (ii) The surface on which probes rest is flat, (iii) the diameter of the contact, between a metallic probe and the sample, is very small compared to the distance between the two adjacent probes.

RESULTS

Fig. 2 shows the plots of resistance of $\text{Bi}_x\text{Sb}_{2-x}\text{Te}_3$ ($x = 0, 0.2, 0.5, 1$) and Fig. 3 shows the plots of resistances of Sb_2Te_3 , $\text{Bi}_{0.2}\text{Sb}_{1.8}\text{Te}_3$ and $\text{In}_{0.2}\text{Sb}_{1.8}\text{Te}_3$ versus temperature, which ranged from 20 K to 300 K. Fig. 4 and 5 show the plots of conductivity of $\text{Bi}_x\text{Sb}_{2-x}\text{Te}_3$ ($x = 0, 0.2, 0.5, 1$) and Sb_2Te_3 , $\text{Bi}_{0.2}\text{Sb}_{1.8}\text{Te}_3$ and

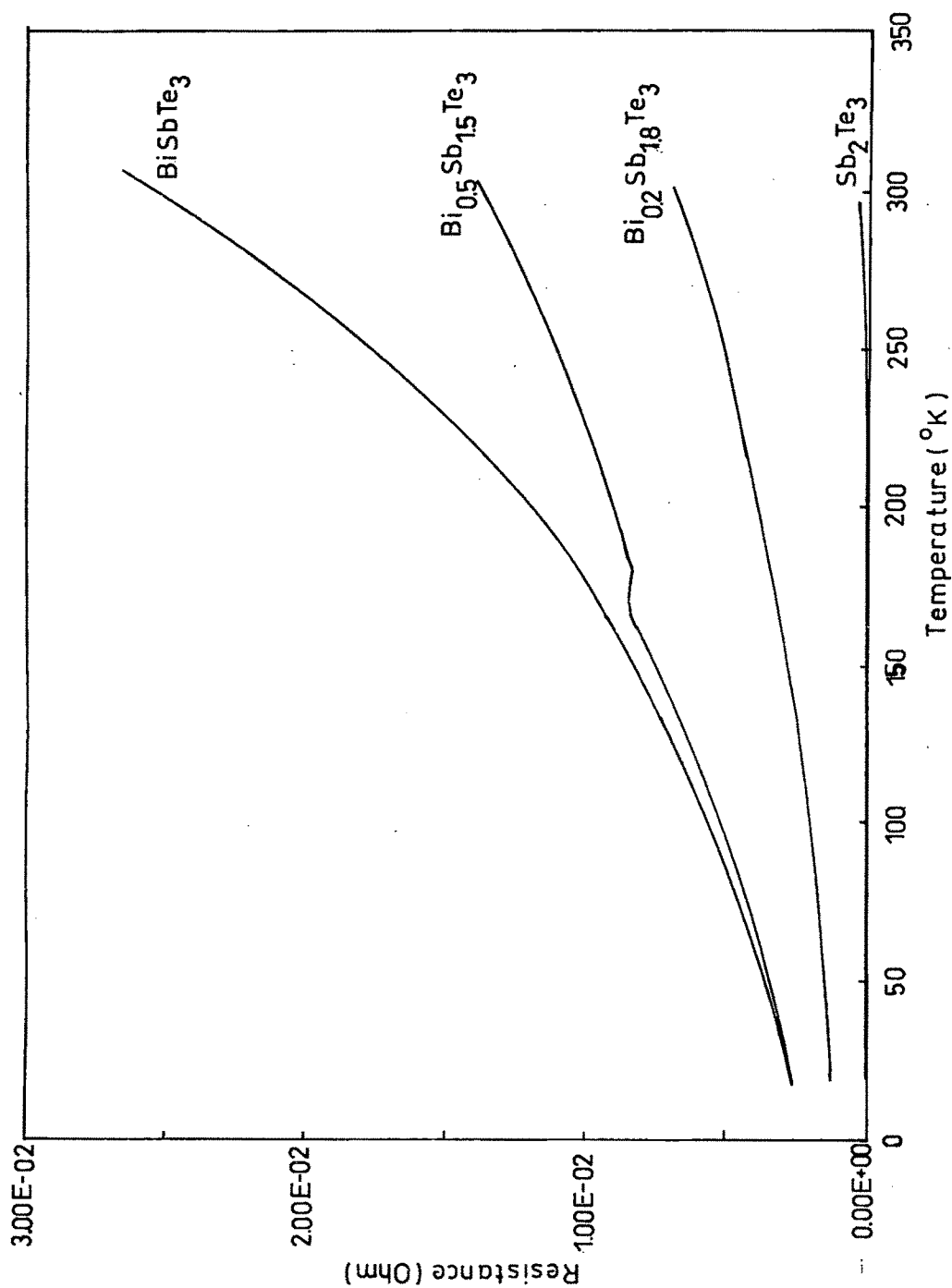


Fig. 2. Plot of Resistance versus Temperature of
 $\text{Bi}_x\text{Sb}_{2-x}\text{Te}_3$ ($x = 0, 0.2, 0.5, 1$)

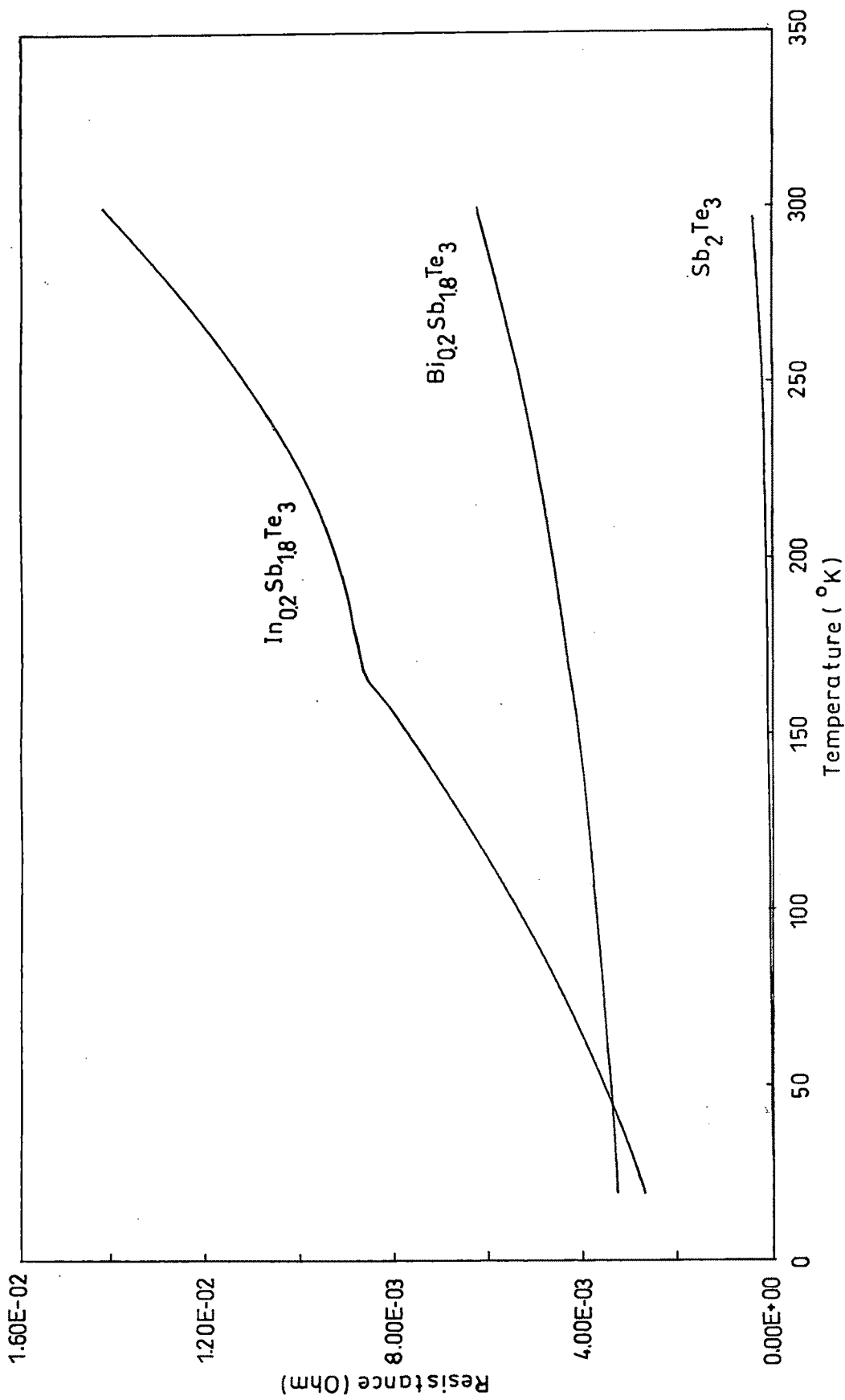


Fig. 3. Plot of Resistance versus Temperature for Sb_2Te_3 , $\text{In}_{0.2}\text{Sb}_{1.8}\text{Te}_3$ and $\text{Bi}_{0.2}\text{Sb}_{1.8}\text{Te}_3$

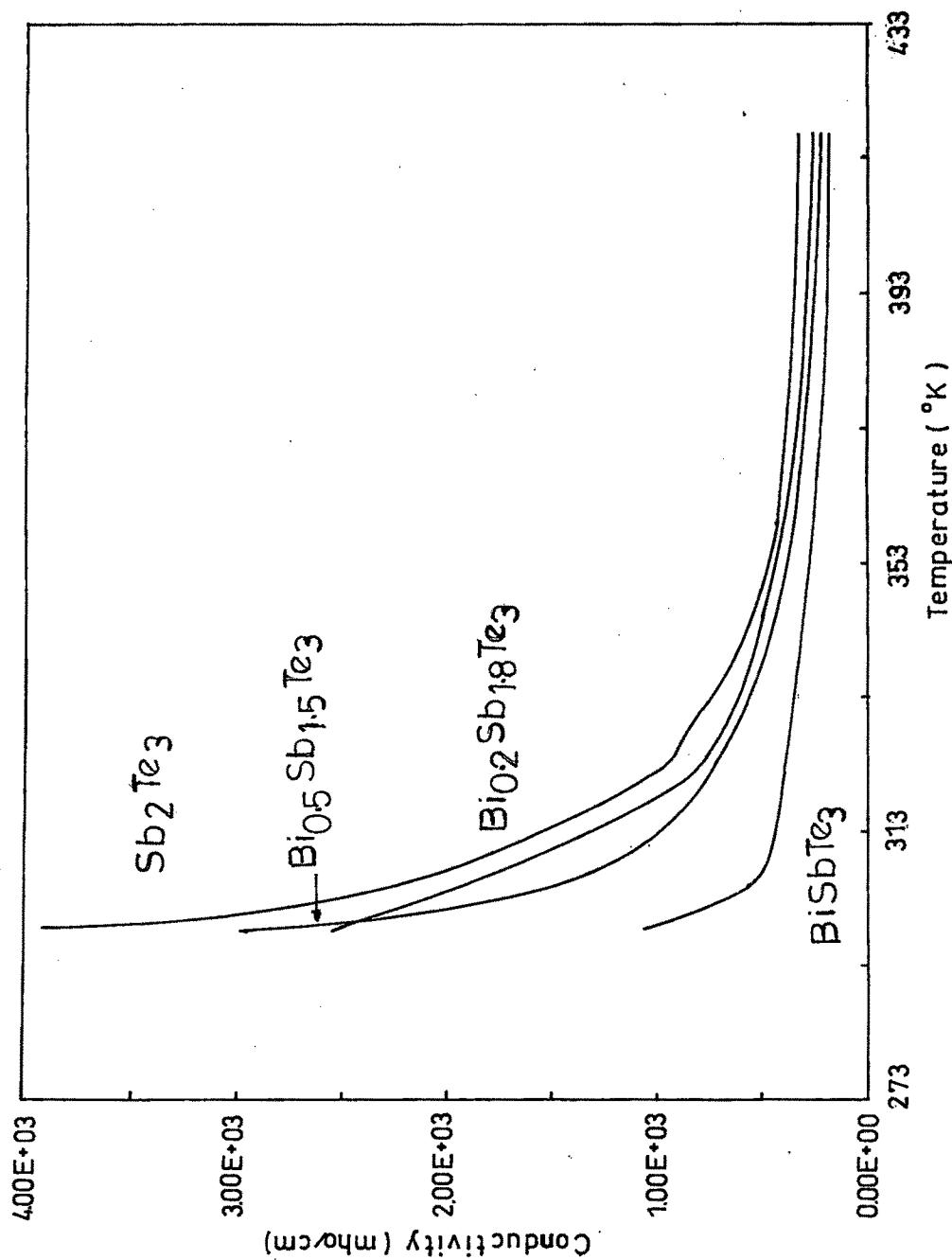
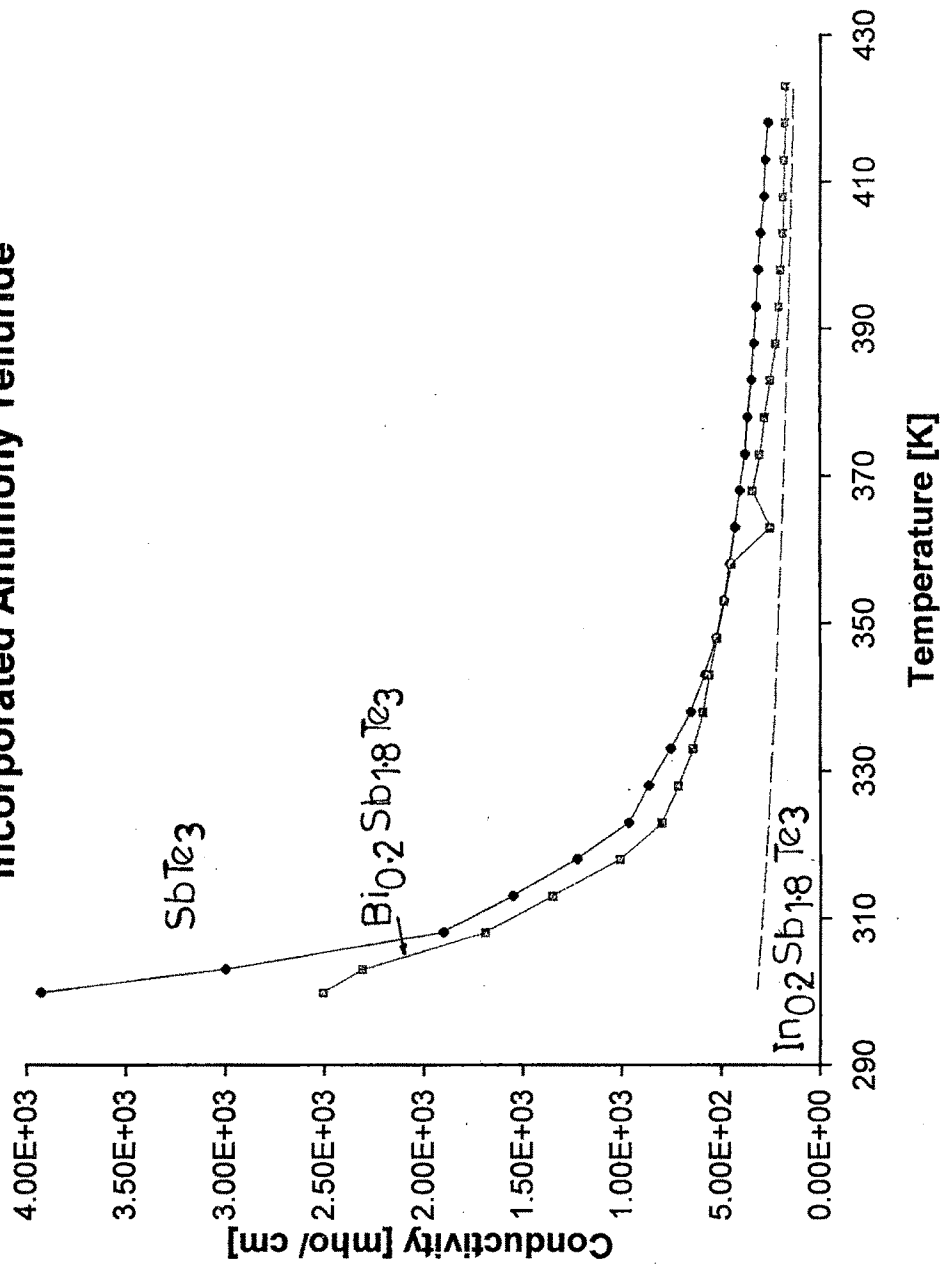


Fig. 4. Plot of Conductivity versus Temperature of $\text{Bi}_x\text{Sb}_{2-x}\text{Te}_3$ ($x = 0, 0.2, 0.5, 1$)

Fig.5 Plot of Conductivity versus temperature for pure and Bi and In incorporated Antimony Telluride



$\text{In}_{0.2}\text{Sb}_{1.8}\text{Te}_3$ against temperature ranging from 298 K to 418 K. It is observed that addition of Bi or In has lowered the conductivity to a significant extent, particularly so, in the case of the In compound except at high temperatures. The results are in trend with those obtained for Sb_2Te_3 : Bi by Jeon et al.^[28] and Zhitinskaya et al.^[29]. The effect can be attributed to the decrease in hole mobility since as per their report, the hole concentration remains practically unaffected. The antisite defects, which are a characteristic of these group V_2VI_3 compounds (caused due to overstoichiometric group V element in the normally crystallized samples), play a major role in suppressing the carrier concentration variation. The transfer of Sb or Bi from its own site to a site normally occupied by Te causes what are known as Sb_{Te} or Bi_{Te} antisite defects. They exist in a concentration to an extent of 10^{19} to 10^{20} cm^{-3} [30-34]. It is known that increase of Bi in $\text{Bi}_x\text{Sb}_{2-x}\text{Te}_3$ induces a decrease in the parent antisite defects Sb_{Te} and this decrease gets compensated by equally participative Bi_{Te} antisite defects which increase with Bi. Hence the hole concentration does not vary significantly. In the case of $\text{In}_x\text{Sb}_{2-x}\text{Te}_3$, the incorporation of In (which is less electronegative than Sb) into the Sb_2Te_3 lattice causes the increase in Sb-Te bond polarity. Hence, not only the antisite defect concentration in this case is very small, but it altogether decreases with an increase in In^[35,36] concentration. Still however, the mobility reduces to a greater extent to dominate the reduction of conductivity^[37].

It is known that $\sigma(T)$ is determined by the temperature dependences of the mobility and carrier concentration. Of the latter two, in the present case as discussed above, the mobility (rather than carrier concentration) variation with temperature has to be provoked to explain the $\sigma(T)$ behaviour. The mobility of the carriers is limited by defect scattering and thermal vibrations of the lattice. Thus the decrease of conductivity with temperature can be attributed to decrease in mobility due to increasing carrier scattering with temperature.

Fig. 6 shows the plot of R^2 versus T^3 (where R is the resistance) for $\text{Bi}_x\text{Sb}_{2-x}\text{Te}_3$ ($x = 0.2, 0.5, 1$), specifically for the lower temperature range. The

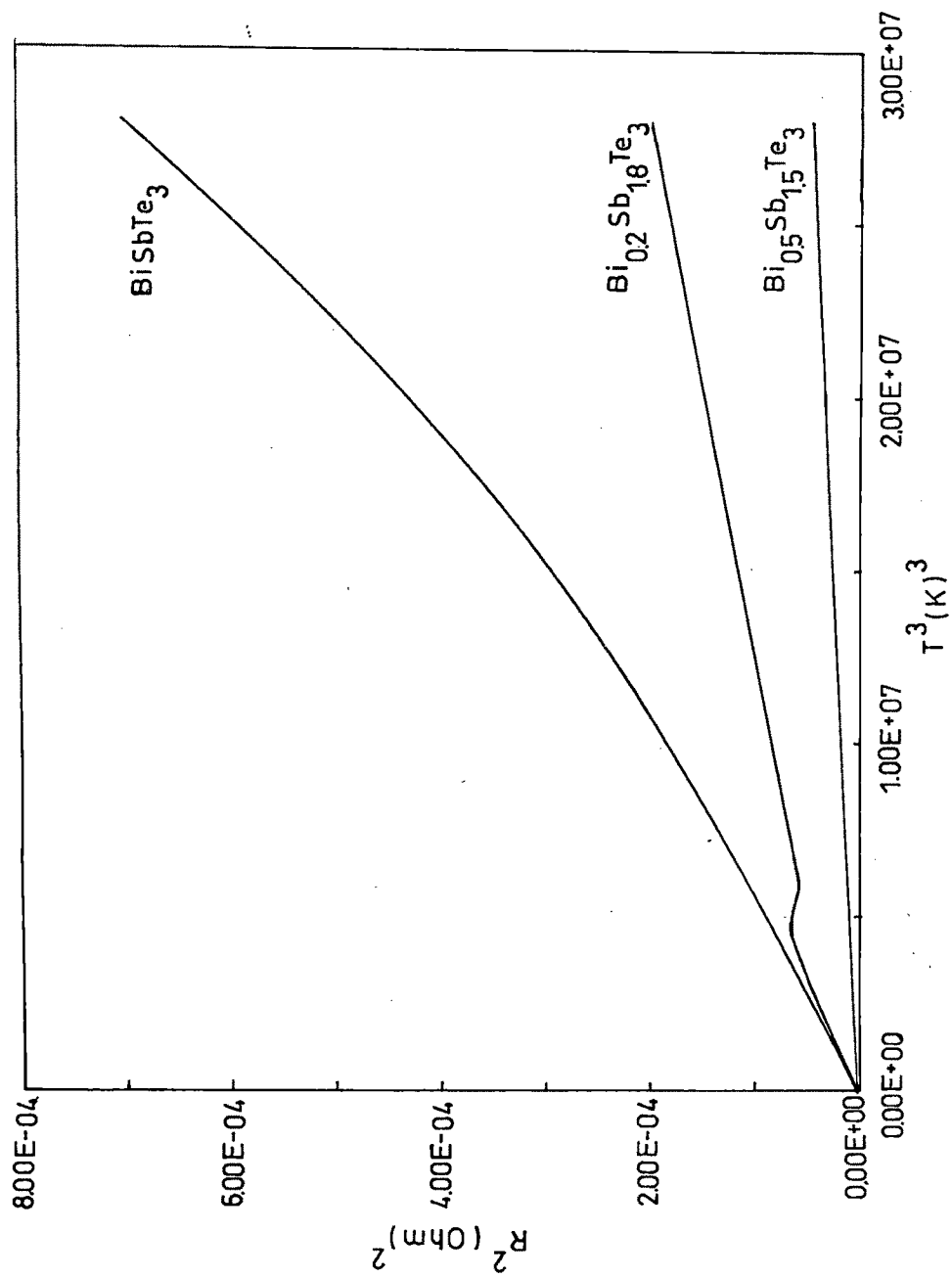


Fig. 6. Plot of R^2 versus T^3 for Bi incorporated Sb_2Te_3 crystals

plots can be seen to follow nearly a straight line trend. This indicates that the acoustic phonon scattering is the dominant scattering mechanism, which must be responsible for reducing the mobility, and hence the conductivity, with temperature. It should however be noted that the small nonlinear nature of the plots may be explained by the hole effective mass changing with temperature as has been done by Ivanova et al.^[14]

Fig. 7 shows the plot of $\log \sigma$ versus $\log T$ for Sb_2Te_3 and $\text{In}_{0.2}\text{Sb}_{1.8}\text{Te}_3$ crystals. In this case as well, the variation of conductivity can be expressed as due to phonon scattering. However, in our investigation the characteristic scattering parameter λ at temperatures above 180K does not correspond to the usual acoustic phonon mode of scattering in the case of Sb_2Te_3 . The parameter has been found to be -1.5, so that the underlying mobility variation would follow T^{1-2} law with $\lambda = -1.5$. This dependence therefore indicates the scattering mode to be two-phonon processes as suggested by E. Gershtein^[38]. Similarly in the case of $\text{In}_{0.2}\text{Sb}_{1.8}\text{Te}_3$, while at the lower temperatures (less than about 180 K) the usual acoustic phonon scattering is obtained, the parameter λ obtained in the range of 1.2 – 1.74, in the higher range of temperatures used, indicates ionized impurity scattering mechanism^[39]. In this respect, it is worthwhile to note that, the impurity scattering has been suggested to increase the Seebeck coefficient and the thermoelectric figure of merit^[40]. This is asserted by the results of thermoelectric power measurements carried out on these materials by the author (as reported in the following section). In these studies, the thermoelectric power has been observed to increase by about 100% as a result of the addition of In. Nevertheless, at sufficiently low temperatures, below about 50K, the conductivity is found to depend but feebly on temperature. This specific feature is usually attributed to complex band structure consisting of two underbands with heavy and light holes^[41]. Thus, the substitutional inclusion of In in Sb_2Te_3 has been found to change the scattering mechanism from simple phonon mode to ionized impurity mode.

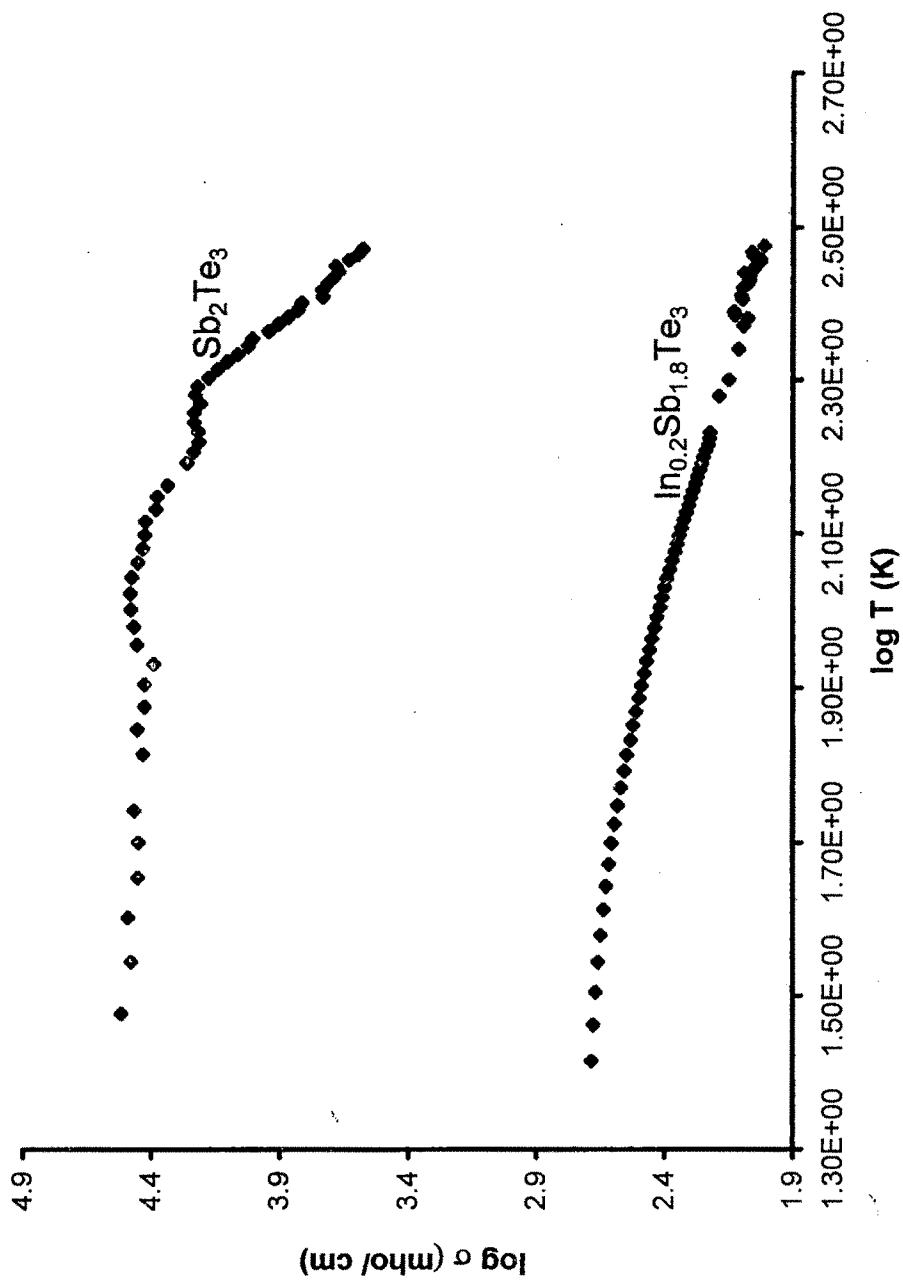


Fig. 7. Plot of log sigma vs log T for Sb_2Te_3 and $\text{In}_{0.2}\text{Sb}_{1.8}\text{Te}_3$

THERMOPOWER STUDY

For these measurements, there are various techniques used by several authors^[42-44]. The present author has used standard differential temperature method for measuring thermopower at different temperatures using the instrumentation described below.

Experimental Set-up:

The Thermopower Measurement System TPSS-200 is a versatile, low cost, specially developed integrated system for measurement of the thermo-emf generated by the "Sample – Stainless Steel probe couple" in presence of a temperature gradient. The experimental system is shown in Fig. 8. It consists of two blocks: 1) sample holder with heaters and pick up probes and 2) electronic circuits controlling temperature and temperature gradient across the sample. The two matched main heaters mounted along the axes of the two sample holder shafts provide the controlled base temperature from 25° C to 200° C. The auxiliary heaters wound on each of the sample holder shafts enable to provide the required gradient upto $\pm 10^\circ$ C. The sign of the gradient can be changed by selecting the auxiliary heater coil A or B. Block 2 consists of temperature indicator, proportional controller and two heater control circuits which drive the two heaters, A and B.

The sample is placed on the sample holder shafts and clamped with the stainless steel probes at both the ends. The microvoltmeter is connected to the output terminal points provided. The temperature is set using the set control knob. If the set temperature is higher than measured T, a power will be delivered to the heater which is proportional to the difference in the set and measured temperatures. The amount of the power delivered is also indicated by the intensity of the lamp that is located near the working space. The temperature stabilizes in about 5-10 minutes. The equilibrium temperature may be lower than the set point and can be adjusted by slightly increasing the bias control knob. The gradient

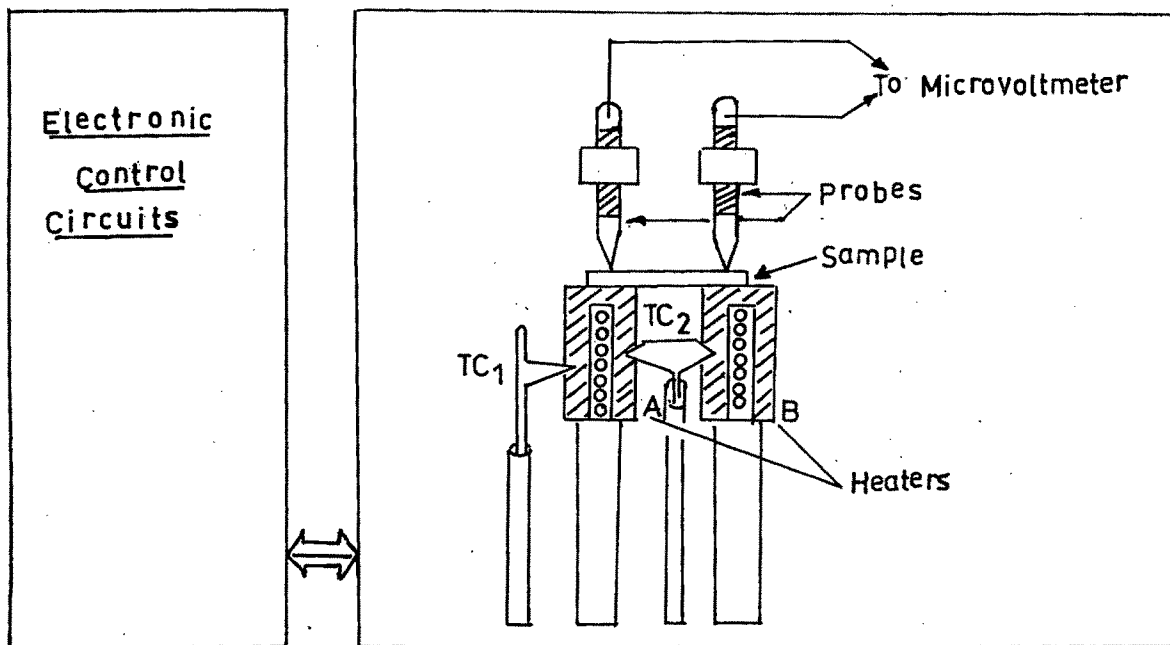


Fig. 8 Thermopower Measurement System

control provides to obtain desired temperature gradient. After the system stabilizes, the readings are obtained.

RESULTS

The Seebeck coefficient S was measured on Sb_2Te_3 crystals with various Bi concentrations and for In incorporated Sb_2Te_3 crystals in the temperature range 25°C to 120°C . For all the samples, the value of S for the direction perpendicular to the cleavage plane was determined. Fig. 9 and 10 show the temperature dependence of the thermoelectric power of pure and Sb_2Te_3 based crystals. The positive sign of the thermoelectric power indicates that antimony telluride is a p type semiconductor irrespective of the kind of doping. This is in confirmation with the results published earlier^[45]. The proportionality of the Seebeck Coefficient with the absolute temperature is the characteristic of the degenerate state and we observe that there is a reduction in degeneracy due to doping of Sb_2Te_3 with Bi or In. This is in agreement with the results reported earlier by Testardi et al.^[46] and Horak et al.^[35].

THERMAL CONDUCTIVITY STUDY

The thermal conductivity measurements are generally done using either a static or a dynamic method. The static method, though more accurate, suffers from the drawback that in addition to the heat conducted through the sample, there are radiative losses from both the heater and the sample to the cooler surrounding and it is also time consuming. The author has used the dynamic method using the instrumentation described below.

Experimental Set-up:

The apparatus used by Ioffe & Ioffe was employed for thermal conductivity measurements and is shown in Fig. 11. The sample is pressed between the copper blocks A and B by means of the screw in the brass bridge. A thin sheet of mica is interposed between the sample and the lower copper block so that the temperature difference between the blocks can be determined by connecting the thermocouples differentially. Glycerine, oil or an amalgam of gallium is used to improve the

Fig. 9. Plot of Seebeck Coefficient versus Temperature of $\text{Bi}_x\text{Sb}_{2-x}\text{Te}_3$ [$x=0, 0.2, 0.5, 1$]

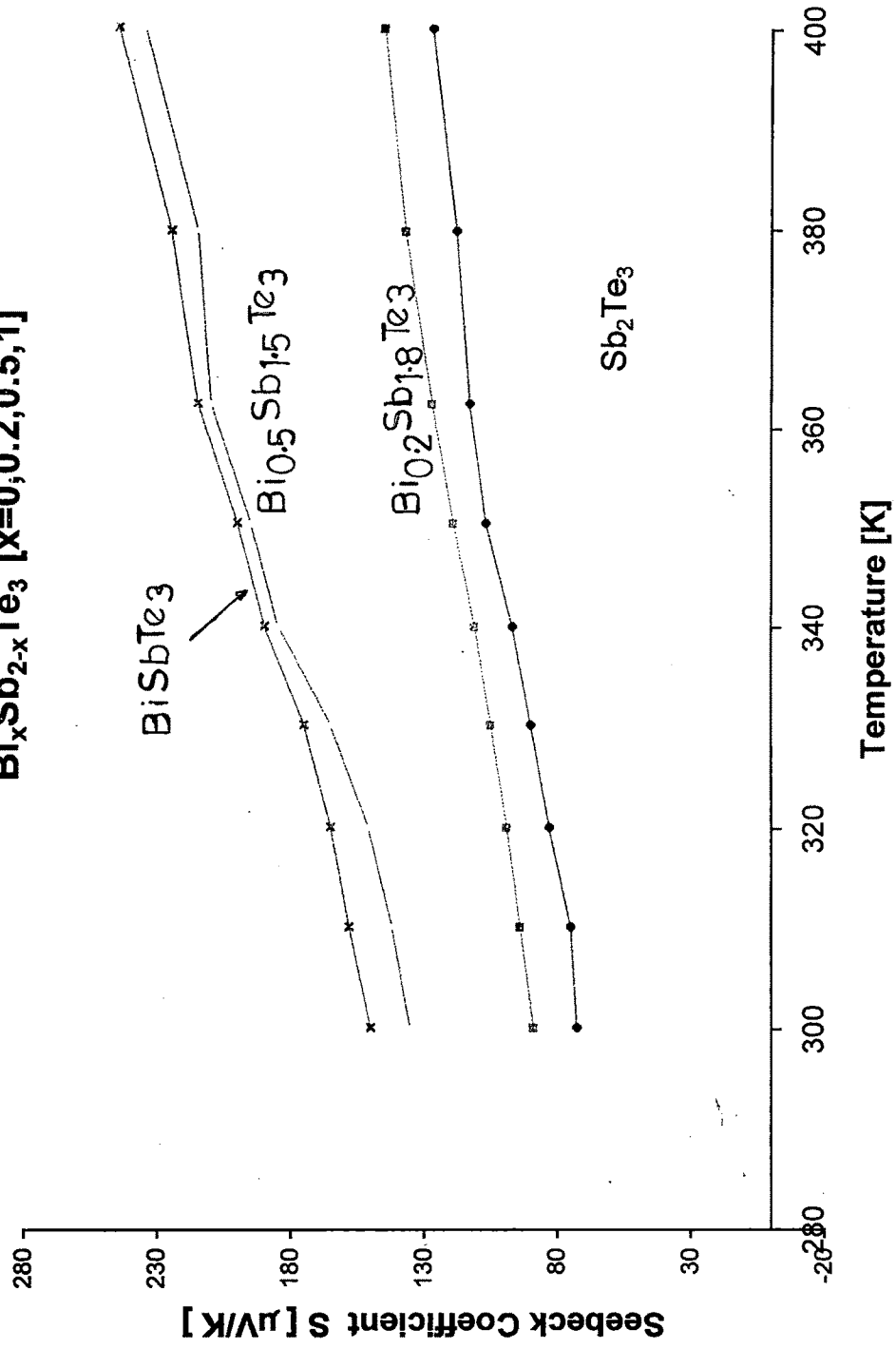
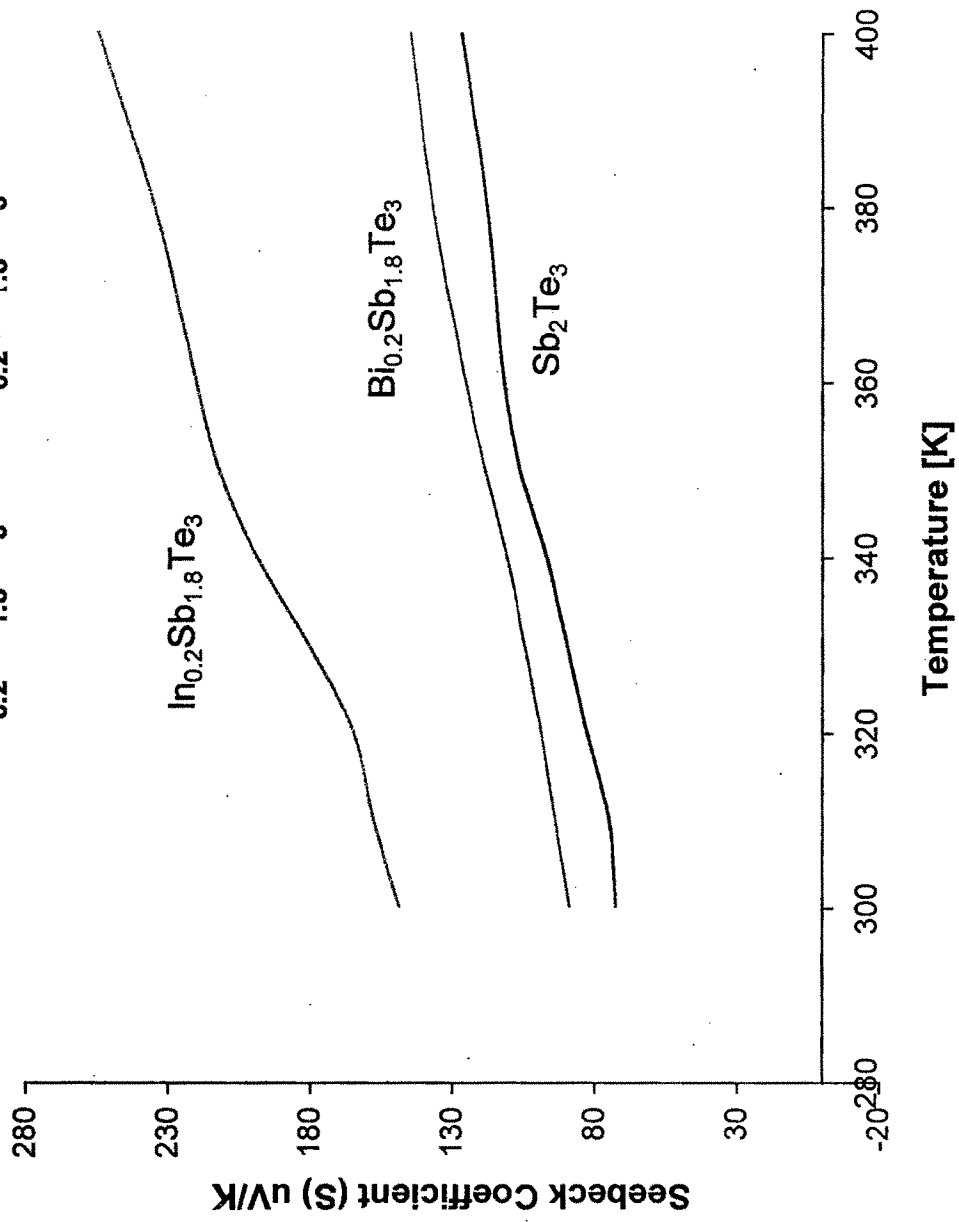


Fig. 10. Plot of Seebeck coefficient versus Temperature for Sb_2Te_3 , $\text{Bi}_{0.2}\text{Sb}_{1.8}\text{Te}_3$ and $\text{In}_{0.2}\text{Sb}_{1.8}\text{Te}_3$



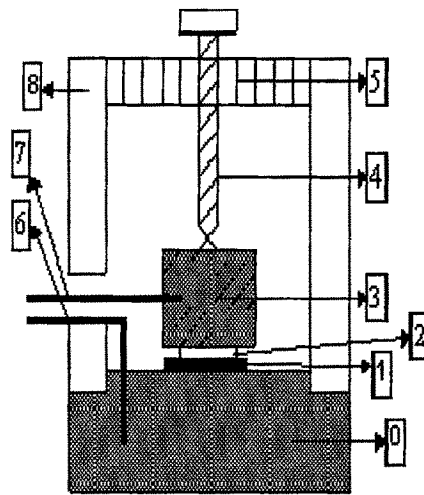


Fig. 11
Ioffe's and Ioffe's Apparatus

- 0. Cu block
- 1. Mica sheet
- 2. Sample
- 3. Cu block
- 4. Screw
- 5. Brass bridge
- 6, 7 Thermocouples
- 8. Methyl methacrylate

thermal contact between the surfaces. Heat transfer between the Cu blocks by way of the screw is obstructed by the poorly conducting perspex walls of the apparatus.

At first the whole apparatus is brought to the same temperature. Then the block A is immersed in a cooling bath and the temperature difference between the blocks as well as the absolute temperature of one of them are continuously recorded. The rate at which heat leaves block B is calculated from its known thermal capacity and its rate of change of temperature. Thus, in principle, the thermal conductivity of the sample may be evaluated from the temperature difference between its ends.

Certain corrections were applied for the errors of measurement not to exceed the figure of 3 to 5% claimed for the method:

- 1) Part of the heat passing into block A originates from the sample itself rather than from block B. Thus one quarter of the thermal capacity of the sample must be added to that of the upper block. However, since the sample is small, it is not necessary to know specific heat of the semiconductor very accurately.
- 2) Another correction must be made for the heat transfer between the upper block and the surrounding walls.
- 3) Allowance must be made for the thermal resistance between the ends of the sample and the thermocouples.
- 4) Transfer of heat between the blocks by convection is small because the lower block is the cooler. It is also reduced by making the space between the upper block and the Perspex walls as narrow as possible.

RESULTS

Fig. 12 shows the cooling curve obtained for the Sb_2Te_3 crystal. The curve was fitted to the equation $y = a e^{-x/b} + c$ where a, b and c are constants. The value of thermal conductivity (κ) of the bulk sample was then calculated using the formula $\kappa = (m s l / A) (1 / b)$; where m is the mass of the upper block, s is the specific heat of copper and A and l are the cross-sectional area and thickness of the sample, respectively. In this method, the error is claimed to be about 5% or

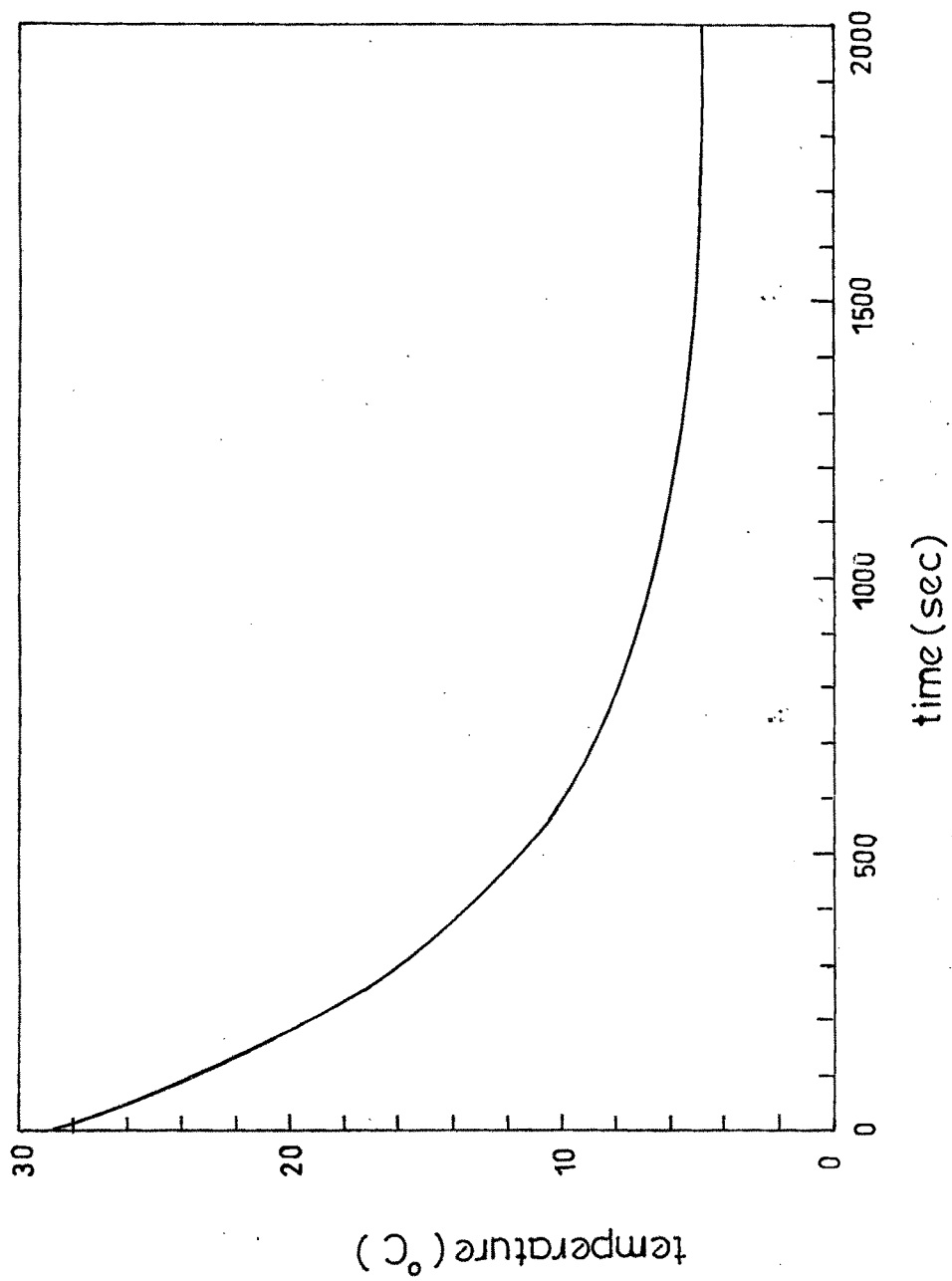


Fig. 12. Cooling Curve of Sb_2Te_3

less. The results are given in Table 1. It is observed that the thermal conductivity of Sb_2Te_3 is in agreement with the result obtained by Herman et al.^[47] who attribute this high value to high electronic component of thermal conductivity in this material.

FIGURE OF MERIT

The early theoretical considerations of A. F. Ioffe et al.^[48] on the thermal conductivity and thermoelectric power of various alloy systems showed that solid solution alloying can result in an improvement in the figure of merit of thermoelements by decreasing the thermal conductivity without affecting the thermoelectric power and electrical resistivity. This is due to distortions of the lattice on alloying which enhance the scattering of phonons, but are ineffective in scattering electrons that have wavelengths longer than those of the phonons. The same phenomena may also be applicable in the present case.

The room temperature values of α , σ and κ and hence the thermoelectric figure of merit, $Z = \alpha^2 \sigma / \kappa$ (α = thermoelectric power, σ and κ = electrical and thermal conductivities, respectively) are given in the Table 1., for various crystals investigated.

It is observed that there is an improvement in the thermoelectric figure of merit of Sb_2Te_3 by addition of bismuth and indium. However, the values do not reach the maximum ($3.3 \times 10^{-3} \text{ K}^{-1}$) reported for the best single crystals of $\text{Bi}_x\text{Sb}_{2-x}\text{Te}_3$ ^[10] single crystal solid solutions. However, by suitable choice of the preparation technique and treatment and addition of a suitable donor, it can be improved.

The results of Indium incorporated Antimony telluride system needs to be pondered upon. It has been observed that the addition of Indium results in reducing the electrical conductivity, increasing the thermopower and decreasing the thermal conductivity.

TABLE 1
Thermoelectric Properties of the Crystals

Crystal	α $\mu\text{V}/^\circ\text{C}$	σ mho/cm	κ $\text{mW}/\text{cm}^\circ\text{C}$	Z $(\times 10^{-3})^\circ\text{K}^{-1}$
Sb_2Te_3	72.70	3937.00	40.72	0.51
$\text{Bi}_{0.2}\text{Sb}_{1.8}\text{Te}_3$	89.00	2502.27	32.85	0.60
$\text{Bi}_{0.5}\text{Sb}_{1.5}\text{Te}_3$	135.20	2985.00	19.68	2.77
BiSbTe_3	150.14	1082.17	28.62	0.85
$\text{In}_{0.2}\text{Sb}_{1.8}\text{Te}_3$	149.00	310.00	7.61	0.90

The present author would like to look at the other aspect of the substitutional effect. Rosenberg et al.^[37] have reported that for $\text{In}_2\text{Te}_3\text{-Sb}_2\text{Te}_3$ solid solutions, with the increase in In concentration, there is a decrease in hole concentration. However, the reduction in mobility is quite larger as compared to the decrease in hole concentration. Hence on the basis of the results obtained, we can say that while In substitutes Sb in Sb_2Te_3 , there is a simultaneous replacement of Te by Sb and it forms a stable InSb compound which has higher mobility^[49]. So, instead of $\text{In}_2\text{Te}_3\text{-Sb}_2\text{Te}_3$ solid solution, it can be said that, rather InSb- Sb_2Te_3 solid solution is formed. Hence there is a strong reduction in the electrical conductivity. In agreement with this finding, we observe an increase in thermopower and reduction in thermal conductivity. This model has its other aspect of explanation through the band gap measurements quoted in the next chapter.

CONCLUSIONS

- 1) All the crystals studied are of p-type as determined by thermopower measurements.
- 2) The addition of Bi and In is found to decrease the electrical conductivity of Sb_2Te_3 . This is explained in terms of reduction of carrier mobility.
- 3) The dominant carrier scattering mechanism in these crystals is of course acoustic phonon scattering. Specifically, the two phonon scattering mode in the case of pure Sb_2Te_3 and the ionized impurity scattering mode in the case of $\text{In}_{0.2}\text{Sb}_{1.8}\text{Te}_3$ are also operative at temperatures above 180 K.
- 4) The thermoelectric figure of merit has been found maximum, viz, $2.8 \times 10^{-3} \text{ K}^{-1}$ for the $\text{Bi}_{0.5}\text{Sb}_{1.5}\text{Te}_3$ crystals, in confirmation with the optimum value possible with these alloys grown in nominal growth conditions.

REFERENCE

- [1] Alieva, T. D., Akhundova, N. M., Barkhalov, B. Sh. and Abdinov, D. Sh. (1991) *Izv. Akad. Nauk SSSR, Neorg. Mater.*, 27, 865.
- [2] Alieva, T. D., Abdinov, D. Sh. and Salaev, E. Yu. (1981) *Izv. Akad. Nauk SSSR, Neorg. Mater.*, 17, 1773.
- [3] Reinshaus, P., Suessmann, H. and Lampe, U. (1993) *Proc. Int. Conf. Thermoelec.* 12th, 49.
- [4] Sussmann, H., Priemuth, A. and Prohd, U. (1984) *Phys. Stat. Sol. (a)* 82, 561.
- [5] Horak, J., Tichy, L., Frumar, M. and Vasko, L. (1972) *Phys. Stat. Sol. (a)* 9, 369.
- [6] Ronnlund B., Beckmann O. and Levy H. (1965) *J. Phys. Chem Solids* 26, 1281.
- [7] Zeinalov, I. A., Askerov, K. A., Aliev, E. M. and Abdinov, D. Sh. (1991) *Izv. Akad. Nauk SSSR, Neorg. Mater.*, 27, 1974.
- [8] Ha, H. P., Cho, Y. W., Byun, H. Y. and Shim, J. D. (1994) *J. Phys. Chem. Solids* 55, 1233.
- [9] Cosgrove, G. J., McHugh, J. P. and Tiller, W. A. (1961) *J. Appl. Phys.* 32, 621.
- [10] Caillat, T., Carle, M., Pierrat, P., Scherrer, H. and Scherrer, S. (1992) *J. Phys. Chem. Solids* 53, 1121.
- [11] Ivanova, L. D., Brovikova, S. A., Sussmann, H. and Reinshaus, P. (1994) *Inorg. Mater.* 30, 716.
- [12] Ivanova, L. D., Brovikova, S. A., Sussmann, H. and Reinshaus, P. (1994) *Inorg. Mater.* 30, 48.
- [13] Ivanova, L. D., Brovikova, S. A., Sussmann, H. and Reinshaus, P. (1995) *Inorg. Mater.* 31, 682.
- [14] Ivanova, L. D., Granatkina, Yu. V., Sussmann, H. and Muller, E. (1993) *Inorg. Mater.* 29, 1093.

- [15] Ivanova, L. D., Granatkina, Yu. V., Sidorov, Yu. A. (1999) *Inorg. Mater.* 35, 34.
- [16] Sherov, P. N. (1987) *Izv. Akad. Nauk SSSR, Neorg. Mater.* 23, 1291.
- [17] Glazov, V. M. and Yatmanov, Yu. V. (1986) *Izv. Akad. Nauk SSSR, Neorg. Mater.* 22, 36.
- [18] Gorelik, S. S., Dubrovina, A. N., Kosheleva, M. N. and Leksina, R. Kh. (1978) *Izv. Akad. Nauk SSSR, Neorg. Mater.* 14, 1051.
- [19] Dik, M. G., Agaev, Z. F., Dubrovina, A. N. and Abdinov, D. Sh. (1987) *Izv. Akad. Nauk SSSR, Neorg. Mater.* 23, 1393.
- [20] Chizhevskaya, S. N., Ivanova, L. D., Svechnikova, T. E., Granatkina, Yu. V., Klim, V. A., Gnatyuk, A. M. and Rozver, Yu. Yu. (1989) *Izv. Akad. Nauk SSSR, Neorg. Mater.* 27, 1194.
- [21] Amin, P. A. A., Al-Ghaffari, A. S. S., Issa, M. A. A. and Hassib, A. M. (1992) 27, 1250.
- [22] Ionescu, R., Jaklovsky, J., Nistor, N. and Chiculita, A. (1975) *Phys. Stat. Sol. (a)* 27, 27.
- [23] Glazov, V. M., Chizhevskaya, S. N. and Glagoleva, N. N. (1967) *Liquid Semiconductors*, Nauka, Moscow.
- [24] Regel, A. R. and Glazov, V. M. (1980) *Physical Properties of Electronic Melts*, Nauka, Moscow.
- [25] Khvostantsev, L. G., Orlov, A. I., Abrikosov, N. Kh. And Ivanova, L. D. (1985) *Phys. Stat. Sol. (a)* 89, 301.
- [26] Aivazov, A. A., Anukhin, A. I., Mazina, A. I. And Boboshko, N. A. (1991) 27, 922.
- [27] Wiese, J. R. and Muldower, L. (1960) *J. Phys. Chem. Solids*, 15, 13.
- [28] Jeon, H. W., Ha, H. P., Hyun, D. B., and Shim, J. D. (1991) *J. Phys. Chem. Solids*. 53, 579.

- [29] Zhitinskaya, M. K., Nemov, S. A., Rykov, S. A. and Ivanova, L. D. (1995) Proc. of 14th International Conference on Thermoelectrics, St. Petersburg, 60.
- [30] Stary, Z., Horak, J., Stordeur, M. and Stolzer, M. (1988) J. Phys. Chem. Solids 49, 191. 45 ref 1,2,3.
- [31] Horak, J., Cermak, K. and Koudelka, L. (1986) J. Phys. Chem. Solids 47, 805.
- [32] Horak, J., Tichy, L., Lostak, P. and Vasko, A. (1976) Crystal Lattice Defects 6, 233.
- [33] Abrikosov, N. Kh., Bankina, V. F., Poretskaya, L. V., Shelimova, L. E. and Skudnova, E. V. (1969) Semiconducting II-VI, IV-VI and V-VI compounds, Ch.III. Plenum Press, New York.
- [34] Brebrick, R. F. (1969) J. Phys. Chem. Solids 30, 719.
- [35] Horak, J., Stary, Z., Lostak, P., and Pancir, J., J. Phys. Chem. Solids, 49, 2, 191 (1988).
- [36] Horak, J., Lostak, P. and Benes, L. (1984) Philosophical Magazine B 50, 665.
- [37] Rosenberg, A. J. and Strauss, A. J. (1961) J. Phys. Chem. Solids 19, 105.
- [38] Gershtein, E. Z., Stavitskaya, T. S., and Stil'bans, L. S., Soviet Physics Tech. Phys. 2, 2302 (1957).
- [39] Goldsmid, H. J. (1964) Thermoelectric Refrigeration (New York).
- [40] Ioffe, A. F. (1957) Semiconductor Thermoelements and Thermoelectric Cooling (Infosearch, London).
- [41] Ronnlund, B., Beckman, O., Levy, H. (1965) Phys. Chem. Sol., 8, 1281.
- [42] Ivory, J. E. (1962) The Rev. Sci. Instr. 33, 992.
- [43] Berglund, C. N. and Beairsto, R. C. (1967) The Rev. Sci. Inst. 38, 66.
- [44] Caskey, G. R. and Sellmyer, D. J. (1969) The Rev. Sci. Instr. 40, 1280.
- [45] Das, V. D., and Soundarajan, N. (1989) J. Appl. Phys., 65, 6.

- [46] Testardi, L. R., Bierly, J. N., and Donahoe, F. J. (1962) J. Phys. Chem. Solids, 23, 1209.
- [47] Harman, T. C., Paris, B., Miller, S. E. and Goering, H. L. (1957) J. Phys. Chem. Solids, 2, 181.
- [48] Ioffe, A. F., Airapetyants S. V., Ioffe, A. V., Kolomoets, N. V. and Stil'bans, L. S. (1926) Dokl. Akad. Nauk. SSSR, 106, 981.
- [49] Sze, S. M. (1979) Physics of Semiconductor Devices, Wiley Eastern Ltd., New Delhi, 20.